

ELECTRIC DISCHARGE STABILIZATION BY A
HIGHLY TURBULENT FLOW

Robert Edward Nelson

Library
Naval Postgraduate School
Monterey, California 93940

NAVAL POSTGRADUATE SCHOOL

Monterey, California



THESIS

ELECTRIC DISCHARGE STABILIZATION

BY A HIGHLY TURBULENT FLOW

by

Robert Edward Nelson

Thesis Advisor:

O. Biblarz

June 1973

T154876

Approved for public release; distribution unlimited.

Electric Discharge Stabilization

by a Highly Turbulent Flow

by

Robert Edward Nelson
Lieutenant, United States Navy
B.S., Tri-State College, 1966

Submitted in partial fulfillment of the
requirements for the degree of

MASTER OF SCIENCE IN AERONAUTICAL ENGINEERING

from the
NAVAL POSTGRADUATE SCHOOL
June 1973

ABSTRACT

This work investigates an electric discharge operating in a turbulent flowing gas. Electric-discharge convection lasers are driven by such a discharge and any limit on discharge power will be a limit on the laser output. It has been observed that turbulence tends to allow more power to be applied but the exact mechanisms involved are not fully understood. To examine this phenomenon an air flow apparatus was fabricated that allowed control of flow rate, turbulence level, and discharge power. Turbulence data were taken with a hot-wire connected to a spectral analyzer. Discharge power consumption and breakdown voltage were recorded as a function of flow rate and turbulence spectrum. Results showed that with even a small flow rate discharge, current was raised by about a factor of two, with turbulence by about a factor of four; and with a large flow rate (100 m/sec) and strong turbulence, by about a factor of 100. Power at this last condition was raised by a factor of 200 over the no-flow case.

TABLE OF CONTENTS

I.	INTRODUCTION-----	7
II.	EXPERIMENTAL APPARATUS -----	11
III.	EXPERIMENTAL PROCEDURE -----	14
IV.	RESULTS-----	17
V.	CONCLUSIONS -----	22
VI.	RECOMMENDATIONS-----	24
	APPENDIX A - MODEL OF THE PHENOMENA -----	46
	APPENDIX B - CALCULATION OF EDDY SIZE -----	48
	BIBLIOGRAPHY -----	51
	INITIAL DISTRIBUTION LIST -----	53
	FORM DD 1473 -----	54

LIST OF ILLUSTRATIONS

Figure

1.	Test Tunnel -----	26
2.	Air Supply Compressor-----	27
3.	Air Supply System -----	28
4.	Detail of Electrodes-----	29
5.	Hot-Wire Anemometer and Oscilloscope -----	30
6.	Spectral Analyzer-----	31
7.	Power Supply-----	32
8.	Laboratory-----	33
9.	Test Tunnel With Hot-Wire Probe-----	34
10.	Box Diagram of Turbulence Data Collection System--	35
11.	Velocity Traverse -----	36
12.	Calibration of RMS Detector-----	37
13.	Sample of Spectral Output-----	38
14.	Sample of Spectral Output-----	39
15.	Spectral Distribution For Screens 3 and 4 -----	40
16.	Correlation of Turbulence Data -----	41
17.	Corona-----	42
18.	General Set-Up For Discharge-----	43
19.	Plot of Current vs Voltage -----	44
20.	Plot of Breakdown Voltage vs Flow Velocity-----	45
21.	Plot of Frequency vs Velocity For $Re(\text{Eddy})=1$ -----	50

LIST OF SYMBOLS

Symbol

A	Area
A_m	Area with mixing
B	Dimensionless parameter
C	Constant
D	Dimensionless parameter
E	Electric field
I	Electric current
I_m	Electric current with mixing
R_e	Eddy Reynolds number
v	RMS value of turbulent velocity component
V_d	Drift velocity
U	Mean velocity
x	Distance downstream of screen
ϵ_0	Permittivity of a vacuum
δ_e	Eddy diameter
δ_{ke}	Eddy diameter based on Reynolds number
ν	Kinematic viscosity
ρ_e	Charge density
ρ_{e_c}	Critical value of charge density
ω	Frequency
ω_e	True frequency of eddy
ω_m	Measured frequency of eddy

ACKNOWLEDGEMENT

The author expresses his sincere appreciation to Assistant Professor Oscar Biblarz of the Naval Postgraduate School, Monterey, California, for his assistance and guidance.

I. INTRODUCTION

The advent of powerful electric-discharge convection lasers (or electro-aerodynamic lasers) has brought about an interest in the dynamics of the gas flow through such devices. The principle of operation of the laser is the transfer of electric power, through a glow discharge, to the vibrational states of nitrogen. This power excites the nitrogen to a higher vibrational temperature and, by collisions, the nitrogen in turn excites or pumps the CO_2 upper lasing level. Any power limit of the discharge thus becomes a power limit of the laser output. As the voltage is increased beyond a critical value, the glow discharge becomes unstable, current fluctuates wildly, and arcs form eliminating the glow discharge. This critical point is a function of the electrode material and geometry, the gas composition, the partial pressures of the gas mixture [4], and the flow turbulence. Since CW operation is desired, it is of interest to raise the arcing voltage to as high a value as possible and to stabilize the current fluctuations. The physics of the lasing process dictate the gas mixture and to some extent the geometry and partial pressures of the constituents. Thus flow conditioning in the form of increased mass flow rates and of turbulence is left as a means of improving the laser output.

Flow conditioning can be broken into two areas, convection and turbulence. Convection removes byproducts that are poisonous to the lasing process. It also removes heat from the electrodes and the discharge cavity. The effects of turbulence are not as well understood. Turbulence is known to extend the breakdown voltage and to stabilize the discharge [2, 6]. It also breaks-up flow discontinuities caused by the introduction of the electrodes in the flowing gas mixture (i. e., it makes the flow more homogeneous).

The study of the dynamics of turbulent flow is a proper field of research by itself. At a given point in a turbulent flow, both velocity and pressure are varying rapidly. This variation is random and can be represented by the sum of a mean term and a fluctuating term. The fluctuating term is defined such that its time average is zero. If this velocity sum is inserted into the Navier-Stokes equations, the resulting equations of motion are similar to those for laminar flow but with extra terms. These extra terms arise from the turbulent fluctuations and are known as apparent, or virtual stresses of turbulent flow (the Reynolds stresses). As long as the relation between the mean and the turbulent components is unknown, the equations of motion cannot be evaluated. This leaves empirical solutions as the best means of analysis.

The concept of an eddy is a useful one in dealing with turbulence. An eddy represents a portion of the fluid that has its own motion.

They are sometimes called "turbulence balls". The maximum possible eddy size is a function of the characteristic size of the flow, such as channel width. Large eddies break up into smaller eddies (cascading). Eventually the eddy size is reduced to the point where viscous effects dissipate them rapidly. Here the Reynolds number based on eddy size is at or below one.

The technique chosen for this work, to study turbulence, is spectral analysis. Spectral analysis uses the distribution of the root mean square of the turbulent energy as a function of frequency to characterize the flow. The density of the spectral distribution may or may not be normalized. With proper equipment, the distribution is not difficult to get experimentally.

The measurement of turbulent flow requires a device with a very rapid response time. The device most commonly used is the hot-wire anemometer. This device functions by inserting a very thin electrically heated wire into the flow. The heat transfer rate of this wire will be a function of the flow velocity. For this work, a constant temperature hot-wire anemometer was chosen for its vastly faster response. The output of the hot-wire, fed through a spectral analyzer, provides the spectral distribution.

The purpose of this work is to investigate the relation between the flow characteristics and the maximum power accepted by a glow discharge operating in such a flow. With sufficient experimental

information of this kind, it is hoped that a model can be formed that will allow the prediction of the discharge characteristics in other flows. This is the beginning of a more comprehensive project which will lead to the CW operation of electric lasers at near atmospheric pressure. The work has been divided into stages, the first of which is the study of electric discharges in flowing atmospheric air.

The working gas chosen for this work was air because this allowed a more careful study of the effects of turbulence on the discharge. While the presence of impurities and of moisture in the air complicate the work, any firm conclusions derived from this work are expected to apply to the normal lasing gas mixture.

Perhaps it is appropriate to restate here that the development of a good discharge for a laser appears to be more of a challenge than the effort required to make a pumped medium lase. At ambient pressures there are a lot of molecules to pump but it is difficult to get a discharge going. About the only thing available is a corona discharge which occurs between a pointed and a smooth electrode. The corona starts when an inception voltage is reached and ends when the gas breaks down into an arc. The current is limited by the mobility of the ions, typically to a few microamps, and is affected somewhat by the flow velocity. The non-uniform electric fields required for corona discharge generally increase with gas pressure or density but the mobility decreases so that the current remains relatively constant.

II. EXPERIMENTAL APPARATUS

The test apparatus was designed for flow speeds around 100 m/sec and variable test section turbulence (Figure 1). Ambient air was supplied by a Carrier three-stage Centrifugal Compressor (Figure 2) with a 4000 ft³/min maximum inlet capacity and a maximum pressure ratio of two. Flow was regulated by a bypass valve venting the main plenum to the atmosphere (Figure 3).

The test section was fabricated of 0.62 cm thick Plexiglas (Figure 1). Plexiglas was chosen for its high dielectric properties, ease of fabrication, and transparency. The electrodes were made of aluminum in a configuration common to many electric-discharge lasers [3] (Figure 4). Originally an electrode separation of 5.9 cm was chosen, but because of power supply limitations it was shortened to 3.9 cm. Also the walls of the test section were slotted to minimize a voltage leakage through the film of moisture that tends to collect on the walls. Hot-wire checks of the boundary layers showed them to be well clear of the pins. Turbulence was introduced by inserting one or more screens upstream of the test section. These screens were mounted in Plexiglas frames and the frames in turn formed a portion of the tunnel. The screens were made of brass, nylon, or phenolic. A pitot tube was used to measure the test section velocity. Barometric pressure was measured with a mercury barometer. Relative

humidity and temperature were measured with a Pacific Scientific Company Model 400 Relative Humidity and Temperature Indicator.

Turbulence measurements were made with a Thermo System Inc. hot-wire anemometer (Figure 5). This consists of a 1051-2 monitor and power supply, a 1054A-30 anemometer module(s), and 1058-6 cabinet. The hot-wire probes were manufactured locally. The output of the hot-wire was connected to a General Radio Company, Type 1921, real time analyzer (Figure 6). The 1921 analyzer consists of a 1925, 30 channel multifilter and a 1926 multichannel RMS detector. The detector processes signals from the multifilter digitally with a variable integration time and storage capacity. The output is read directly on Nixie tubes, one channel at a time. A Hewlett-Packard X-Y Recorder was connected to the detector to provide a rapid graphic output of the spectrum; the data were also manually recorded. The hot-wire probe was introduced through holes in the side of the test section. Entry was also made through the end of the tunnel but this proved less desirable as many wires were broken in this way. The transparency of the Plexiglas allowed the operator to place the probe in areas of interest by visual means, thus saving much traversing equipment. A Tektronix oscilloscope was connected to the hot-wire for initial set up and to provide a continuous monitor of the hot-wire operation.

The electric-discharge power was furnished by a Sorensen High Voltage D. C. power supply (Figure 7). This unit has an output of up to 30 kV D. C. and 20 ma with a 2% ripple. Trip controls work on both current and voltage. The high voltage was measured with a Sensitive Research electrostatic voltmeter with a capability of a 40 kV and an internal impedance of 5×10^{15} ohms. Current measurements were made with various microammeters and milliammeters. As the magnitude of the current covered many decades, current was difficult to measure. The most satisfactory method was to connect a microammeter and a milliammeter in series and short out one when out of its range.

High voltage connections were made on polished brass balls approximately 2 inches in diameter. All leads were made of high-voltage wires. The laboratory has its own grounding system and great care was taken to ensure proper grounding of all equipment. When the high voltage power supply was activated, all unnecessary equipment was secured and electrically isolated.

Figure 8 shows the general laboratory set up. The compressor and air bleed valves are not shown in this picture but the tunnel and electronic equipment are visible. Figure 9 shows the hot-wire probe inserted in the test section. Shot bags help secure the traverse mechanism. Figure 10 shows a box diagram of the turbulence data collection system.

III. EXPERIMENTAL PROCEDURES

The procedure was broken down into three phases: design and fabrication, turbulence measurements, and electric discharge measurements. As work progressed, new information made it necessary to return to one or more of the previous phases.

The nature of this work required long run times. Because of this, it was decided to use ambient air as the working gas. As there was no satisfactory means to dry the air, relative humidities from 10 to 50 percent were encountered during the various runs. These values were recorded so that humidity effects could be taken into consideration.

The hot-wire was, at all times, set up for maximum frequency response. The following procedure was used to achieve this: all set-up work was done with the probe in the maximum flow velocity expected for that day's series of runs. The STABILITY control was set full clockwise and then turned back until the output was stable with TRIM full counter-clockwise. Then the TRIM control was turned clockwise until an oscillation occurred, and then turned back slightly past the position required to stabilize the output. To check stability, the built-in 1 kHz and 20 kHz signals were temporarily switched in. The linear output control was set at or near 9.0 for the maximum flow condition.

Hot-wire probes were manufactured locally. The wires were made up from .00015 in. diameter tungsten. As a solder joint cannot be made to tungsten, the wire was copper plated at the solder joints. A ten-power binocular microscope was required when soldering the wires to the probes.

Hot-wire measurements were first used to examine the flow characteristics in the test section. This showed the velocity and the turbulence spectrum to be reasonably uniform throughout the discharge portion (Figure 11). It is of interest to notice that introduction of the hot-wire probe reduced the tunnel cross-sectional area enough to alter the velocity, very slightly, between the left and right portions of the profile. Because of the uniformity, subsequent measurements were taken at the center point only. To check for homogeneity, the wire was rotated 90 degrees and the spectral output data showed no significant changes. At this point, turbulence surveys were made using each screen and various velocities. The no-screen spectrum was also surveyed.

Next the discharge work began. Current measurements were initially made with microammeters, but as the work progressed it became necessary to switch to milliammeters. Breakdown of the discharge was considered to occur when an arc formed with the accompanying vast increase in current and subsequent power supply shut-off.

As the voltage used was as high as 30 kv, great care was taken to prevent injury.

The RMS detector of the real time analyzer was calibrated (Figure 12) by the introduction of a known 5 kHz signal. Calibration was done with the CAL control set at -12 DB and all the attenuators set at -10 DB.

IV. RESULTS

Spectral measurements of the turbulence (existing) in the test section were made. Figures 13 through 15 show examples for various flow configurations. These figures are tracings of the output of the X-Y plotter. The low frequency spikes are noise from outside of the system and do not reflect values existing in the flow. Screen (1), consisting of 20 wires/cm, produced turbulence levels very similar to the no-screen case but with less turbulence in the low frequency range and slightly less in the higher frequencies (for the same velocities). Screen (2), consisting of 7.3 wires/cm, produced turbulence peaks between 2.5 kHz and 6.3 kHz. The last configuration used consisted of a phenolic plate (4) with a large number of 0.635 cm holes mounted with screen (3), which had 7.3 strands of nylon per cm. This produced peaks between 1.25 kHz and 6.3 kHz but with more energy in the lower frequencies (i. e., larger eddies). This distribution was very similar to the no-screen case but was achieved with less velocity, an important factor.

Turbulence was found to exist under all flow conditions, including the no-screen case. This case showed more of the lowest frequency (below 200 Hz) turbulence than any of the screen cases. Where a screen was mounted, a shift to the higher frequencies occurred, but at high enough frequencies (above 2.5 kHz) the readings with and without screen became similar.

The maximum of the spectral distribution can be thought of as the point where the eddy Reynolds number is about one. At this value, the viscous forces are as important as the convective forces acting on the eddies. The theory set forth in Reference 1 predicts that, for a given flow situation, turbulence will first fill out the lower frequencies. As more turbulence is introduced, the turbulence level in the lower frequencies will remain constant and the added energy will cause the peak to shift to higher values (in frequency and in strength). To summarize, as turbulent energy is added it will cause the higher frequencies of the spectral distribution to fill out. This pattern was clearly present in the spectral data taken, which closely resembles the pattern shown in Figure 7.6 of Reference 1. At very low velocities the turbulence was (typically) dissipated by 12.5 kHz with a peak at 1.25 kHz. At high flow rates the turbulence was far from dissipated at 20 kHz (the limit of the analyzer) and had a peak at 6.3 kHz (Figure 14).

When a dimensionless parameter, D , which has the form of a Reynolds number, and a dimensionless velocity, B , are defined as

$$D = \frac{V^2}{\omega \nu} \quad \text{and} \quad B = \frac{X \omega}{U}$$

the following relation is found to hold

$$B = CD^{-0.47} \quad R_e < 1$$

Figure 16 shows this effect with various velocities and screens plotted on one curve. When the value $R_e \doteq 1$ was reached the relation broke

down; hence the data are representative of homogeneous turbulence only.

An order of magnitude analysis was made of the eddy size present in the flow (see Appendix B). This showed the eddies to be very small (5×10^{-4} mm at 8 kHz and 5×10^{-2} mm at 200 Hz). The amount and size of the eddies are important when attempting to understand the effect of turbulence on the electric discharge. As a check on the accuracy of the analysis, the eddy size at the $R_e = 1$ point was calculated and compared with the eddy size from the definition of Reynolds number; the check showed the analysis to compare within an order of magnitude.

The electric discharge formed a corona when an inception voltage was reached in the flowing gas (Figure 17). Figure 18 shows the set-up for the discharge work. The corona started as a small conical yellow-blue spray emitting from the pins (anodes). As the voltage was raised slightly this moved to all the pins and became longer. Eventually the spray joined at about one cm downstream. At this point the corona was blue violet in color. As the voltage was raised the corona became more intense but tended to become unstable and to break down into an arc. A very small corona formed when the air was not flowing. The onsets of corona breakdown and of arcing are very close together in still air.

Discharge power consumption results are shown in Figure 19. The no-flow case had a maximum current of about 50 μ a at 23.5 kV. Typically the maximum voltage for this case was much closer to 22 kV with a current of 30 μ a. It is felt the scatter was caused by changes in humidity which tend to increase the breakdown voltage. [4] For comparison the following current and voltage data were taken from runs where the velocity was between 60 and 65 m/sec: with no screen, the maximum current was on the order of 80 μ a at 24.2 kV, with screen(2) the maximum current was on the order of 70 μ a at 24.7 kV, and with screens (3) and (4) used together maximum current was on the order of 300 μ a at 26 kV. When the velocity was increased to 72 m/sec and screens (3) and (4) operated together maximum velocity with this configuration) the current was 9 ma at 26 kV. With velocity increased to 96 m/sec and using screen (2), the current was 11 ma at 24.5 kV. These runs were made on different days. Note the power for the no-flow case is about 1.2 watts, whereas the maximum power achieved was on the order of 270 watts at the high flow rates.

Breakdown voltage also varied with velocity and turbulence, but not as markedly as power (Figure 20). With no flow, the breakdown voltage varied between 21.5 kV and 24 kV, with a mean between 22 kV and 23 kV. With no screen mounted, the flow did not significantly raise the breakdown voltage; for all velocities it remained between

22.4 kV and 24.2 kV. With screen (2) mounted it went as high as 26 kV (for 97 m/sec), the mean being above the no flow case. With screens (3) and (4) mounted together, breakdown rose as high as 26 kV (for 76 m/sec) and remained well above the no-flow case.

V. CONCLUSIONS

The data presented in this thesis confirm that a turbulent flow does in fact stabilize an electric discharge and allows it to accept more power. Two effects appear to be taking place: mixing due to turbulence and convection, convection being the lesser in importance.

Pure laminar flow was not achieved, and thus it is difficult to separate convective effects from mixing effects. However, when turbulence was not introduced into the flow by the screens and when the velocity was below 50m/sec, the mixing effect was considered to be small. Under these conditions even small flows tended to increase the current by a factor of two over the no flow case. Break-down voltage, however, did not increase significantly until 50 m/sec flow velocity was exceeded (Figure 20). At the higher flow rates turbulence, originating at the plenum, was starting to appear.

Turbulent mixing had a strong effect on both current and break-down voltage. Examination of Figure 19 shows that current was raised to as much as 11 ma (here, at times, the capability of the power supply may have been exceeded). It is felt that the most useful turbulence is that between 1 kHz and 10 kHz. A further requirement is that the turbulence must be intense throughout this range. Screens (3) and (4) mounted together produced such a spectral distribution.

With this combination a current of 9 ma was achieved with a velocity of 60 m/sec. With screen (2) or (3) the spectrum had a peak in the high frequency range but very little energy in the lower region. With these screens, velocities of up to 97 m/sec were needed to achieve currents in the 7-11 ma range. The spark breakdown voltage was raised by turbulence, at all flow velocities used, by an average of 2 kV. All screens increased the breakdown value (26 kV being the maximum) but screens (2) or (3) required velocities in the 90 m/sec range to do this (i. e., the lack of large eddies shows up as an increased velocity need). Screens (3) and (4) used together produced this in the 20 m/sec range.

Several other conclusions are made. First, the arcing voltage increased with relative humidity. This effect was expected [4]; no attempt was made to adjust the data for it. Second, the turbulence data follow some of the anticipated trends and this lends confidence to the work. And, third, metal screens seemed to have no effects differing from those of similar nonconduction screens.

VI. RECOMMENDATIONS

The spectral data proved useful in this work. But it is felt that their value would be far greater if the analyzer output was taken in a form suitable for direct computer input (i. e. , magnetic or paper tape). This would allow rapid calculation of parameters of interest. Also, this would serve as a permanent record with rapid data retrieval capability.

It is recommended that the method of introducing turbulence to the flow be changed. The drawback with screens is the difficulty in generating large eddies. It is felt that a series of adjustable baffles used in conjunction with screens could achieve this. The baffles might be arranged in two rows normal to each other. Also it might be of interest to arrange the baffles so that their number can be changed.

A great deal of flow time was consumed while the power supply was adjusted for the desired voltage. Two other problems occurred with the power supply: insufficient voltage and power. For these reasons it is felt that consideration should be given to replacing it with one more suitable for this work. A power supply capable of producing accurate voltage as selected, and across a wide band, would be of particular value.

Current measurements proved to be difficult. It is felt that this work would profit from an ammeter capable of automatically switching ranges without disturbing the discharge.

The next step in this work should be the building of a closed system where the flow constituents can be controlled. An appropriate CO_2/N_2 mixture could be used in such a system, eventually leading to a lasing demonstration.

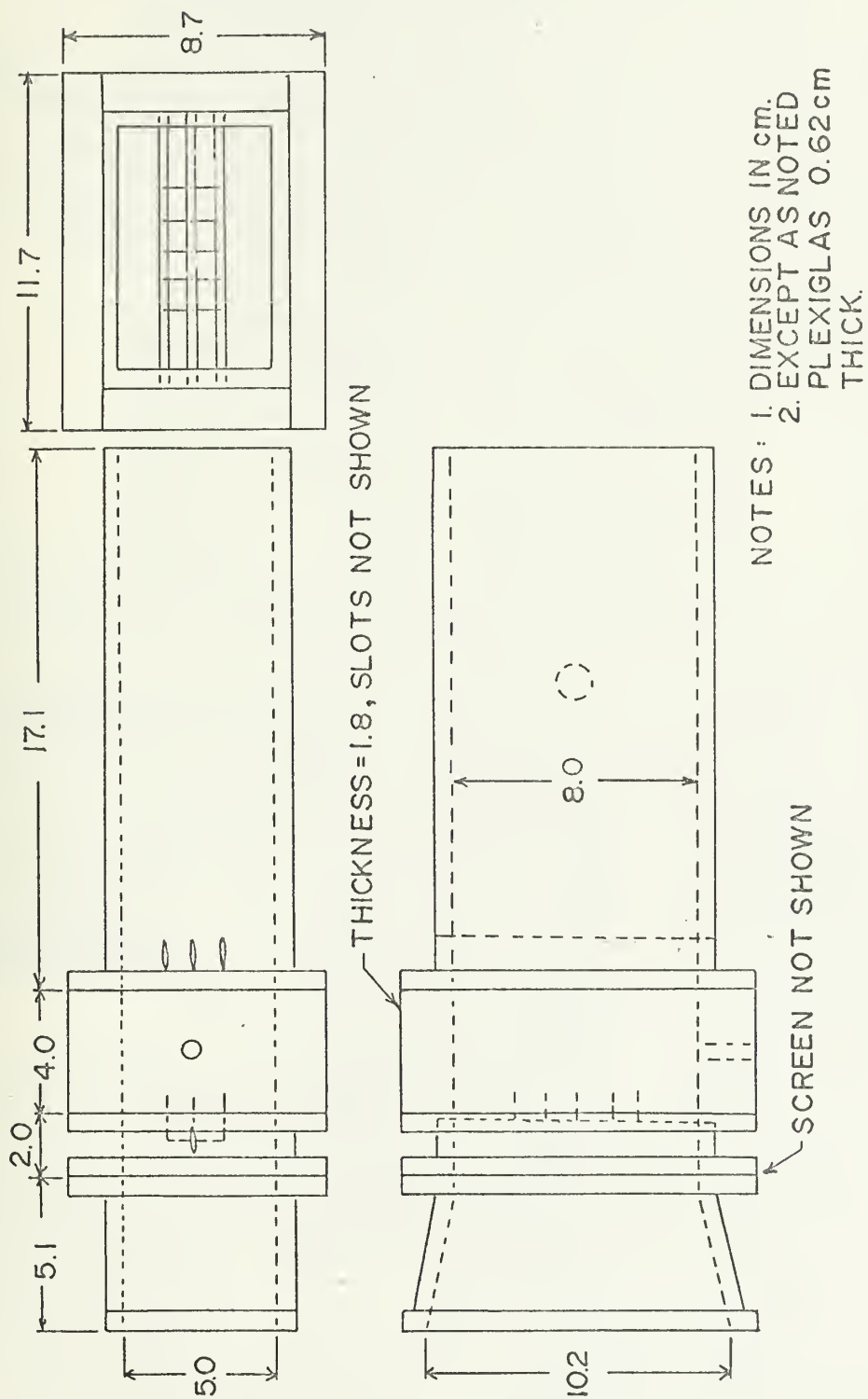


FIGURE I. TEST TUNNEL

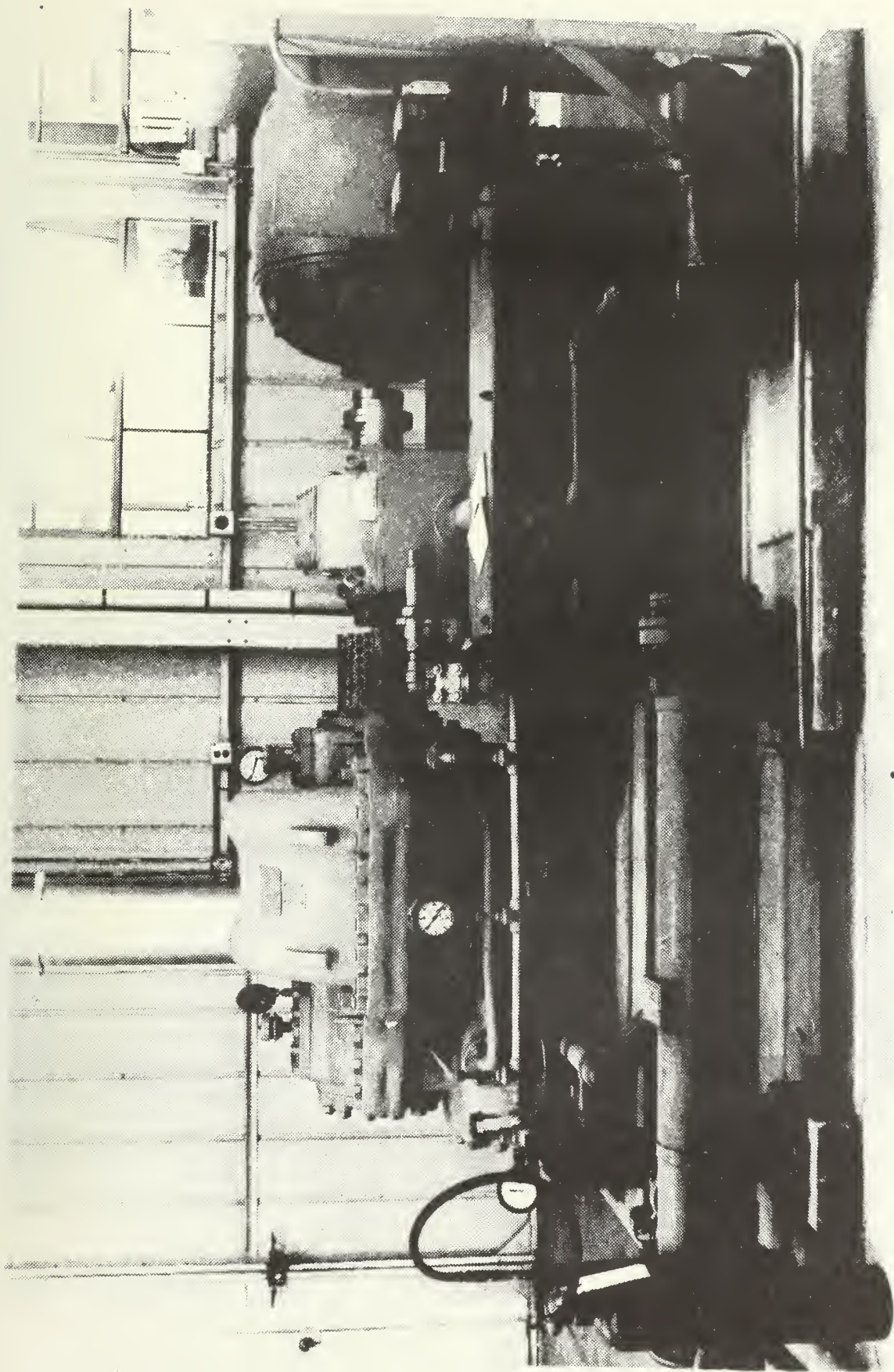


FIGURE 6. AIR SUPPLY COMPRESSOR

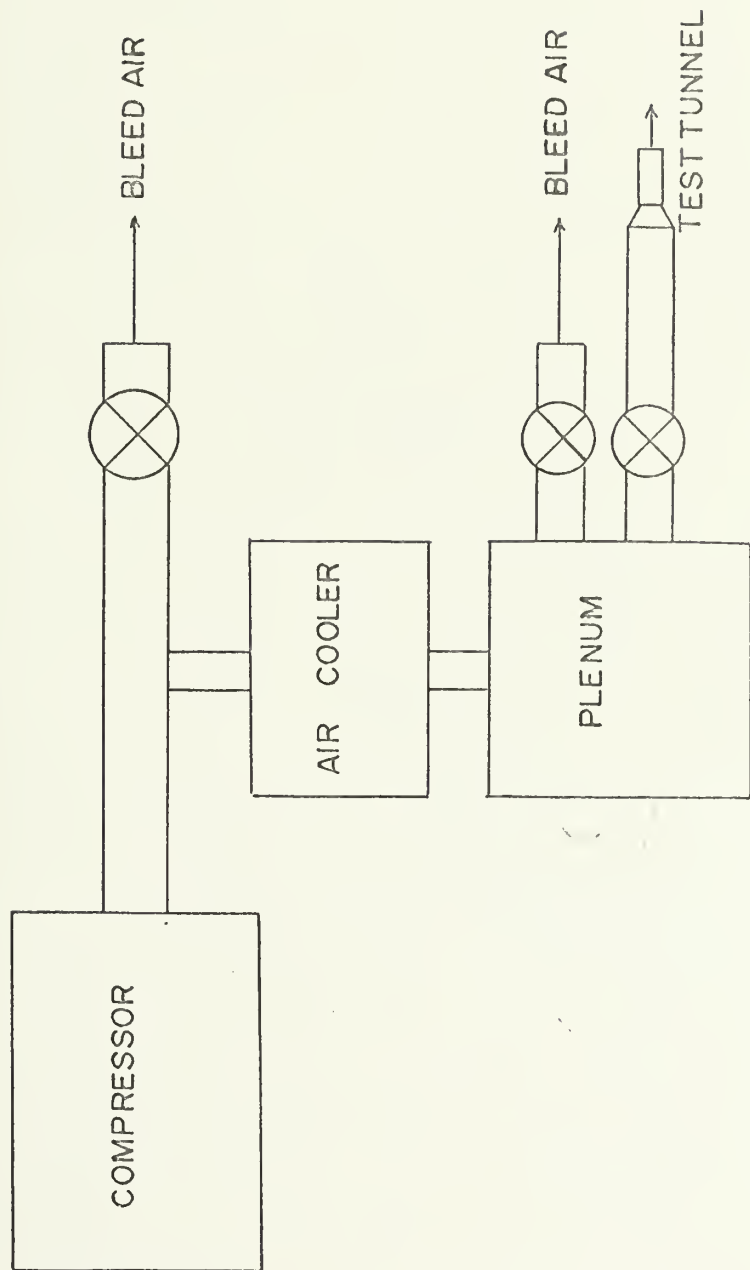


FIGURE 3. AIR SUPPLY SYSTEM

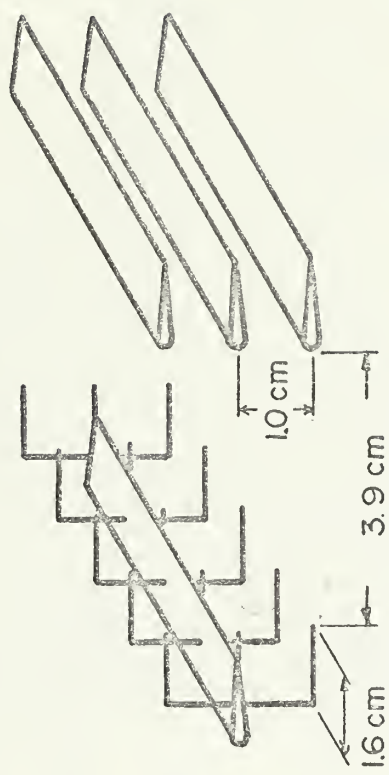


FIGURE 4. DETAIL OF ELECTRODES

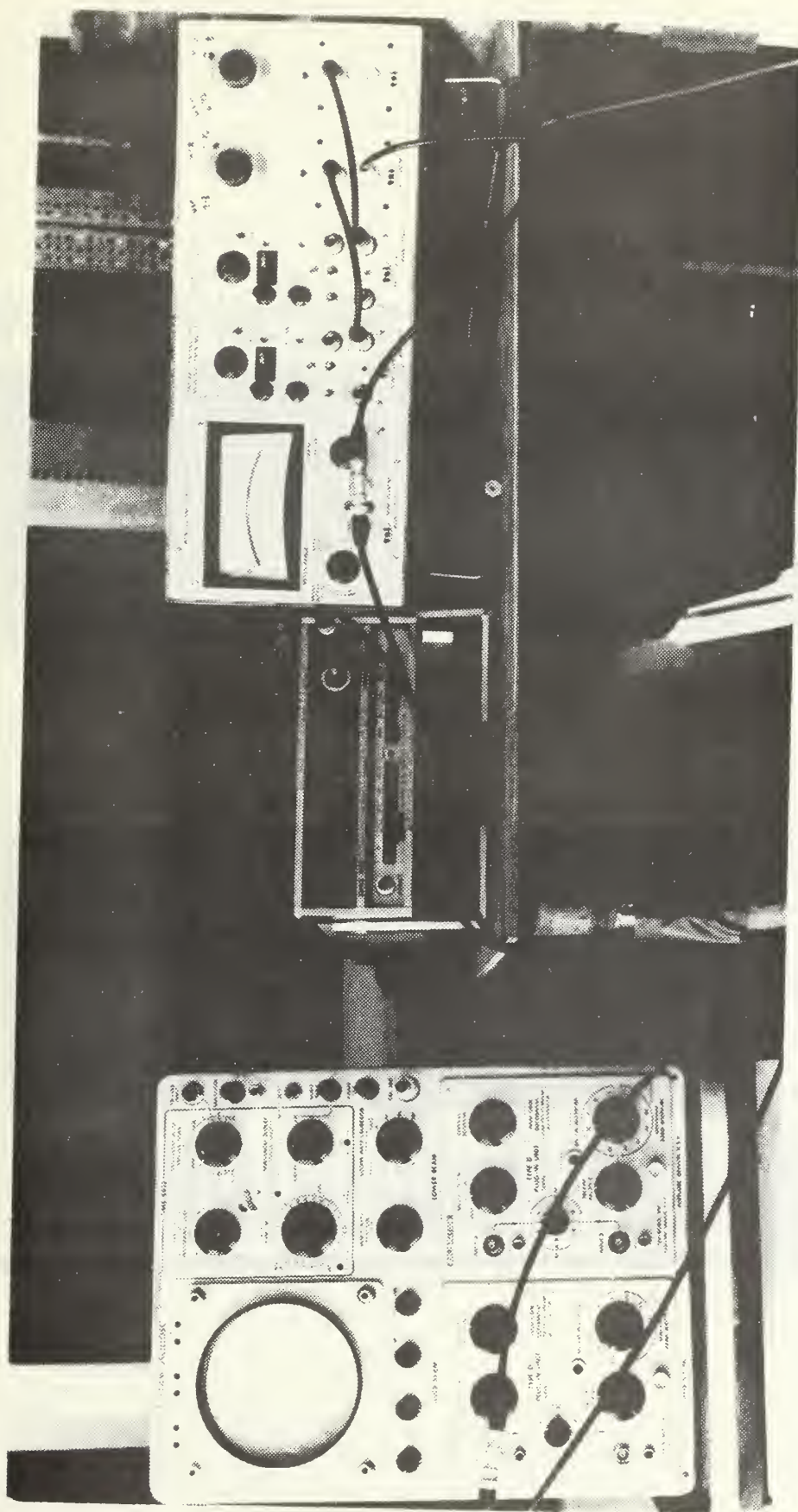


FIGURE 5. HOT-WIRE ANEMOMETER AND OSCILLOSCOPE

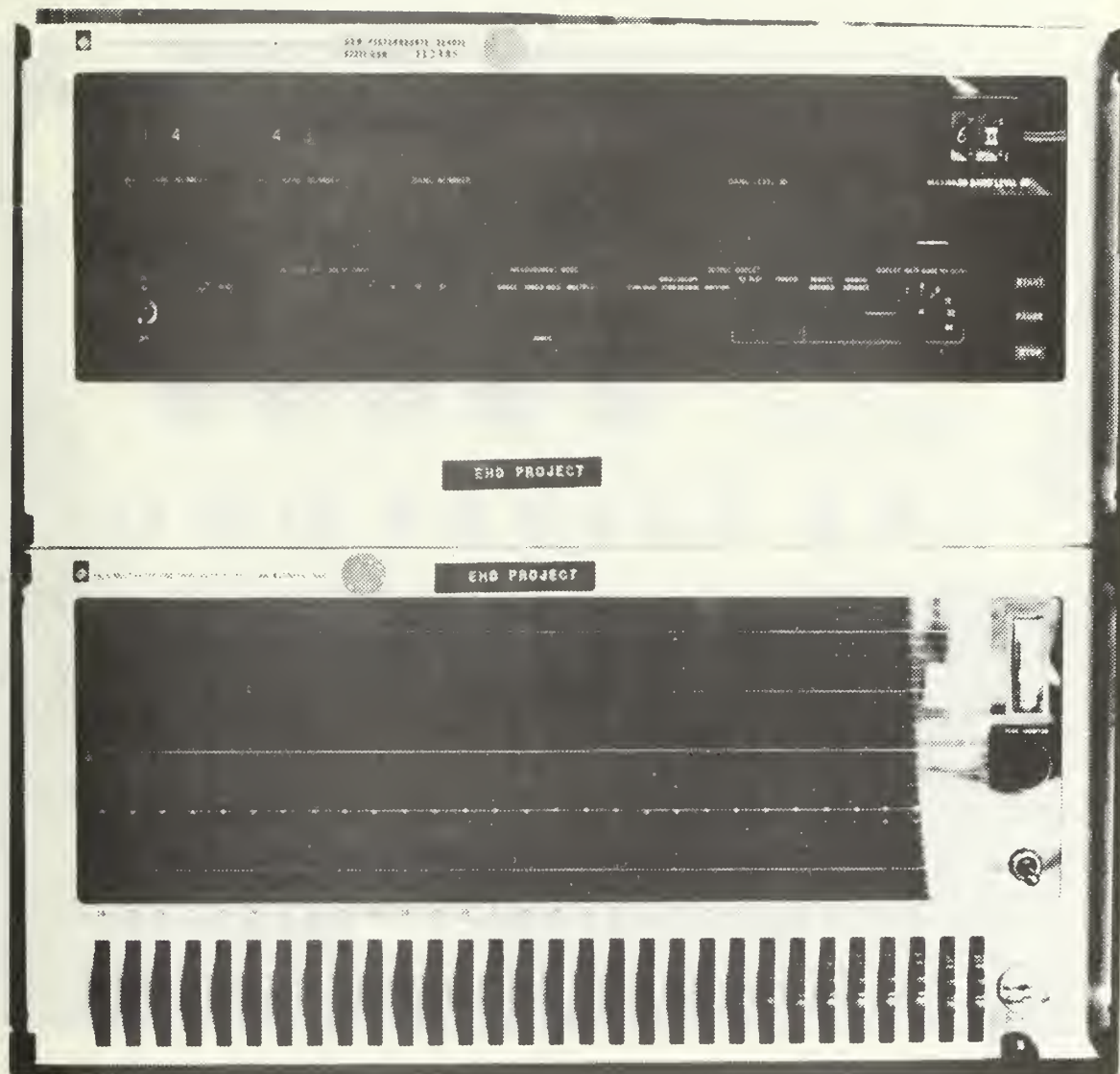


FIGURE 6. SPECTRAL ANALYZER

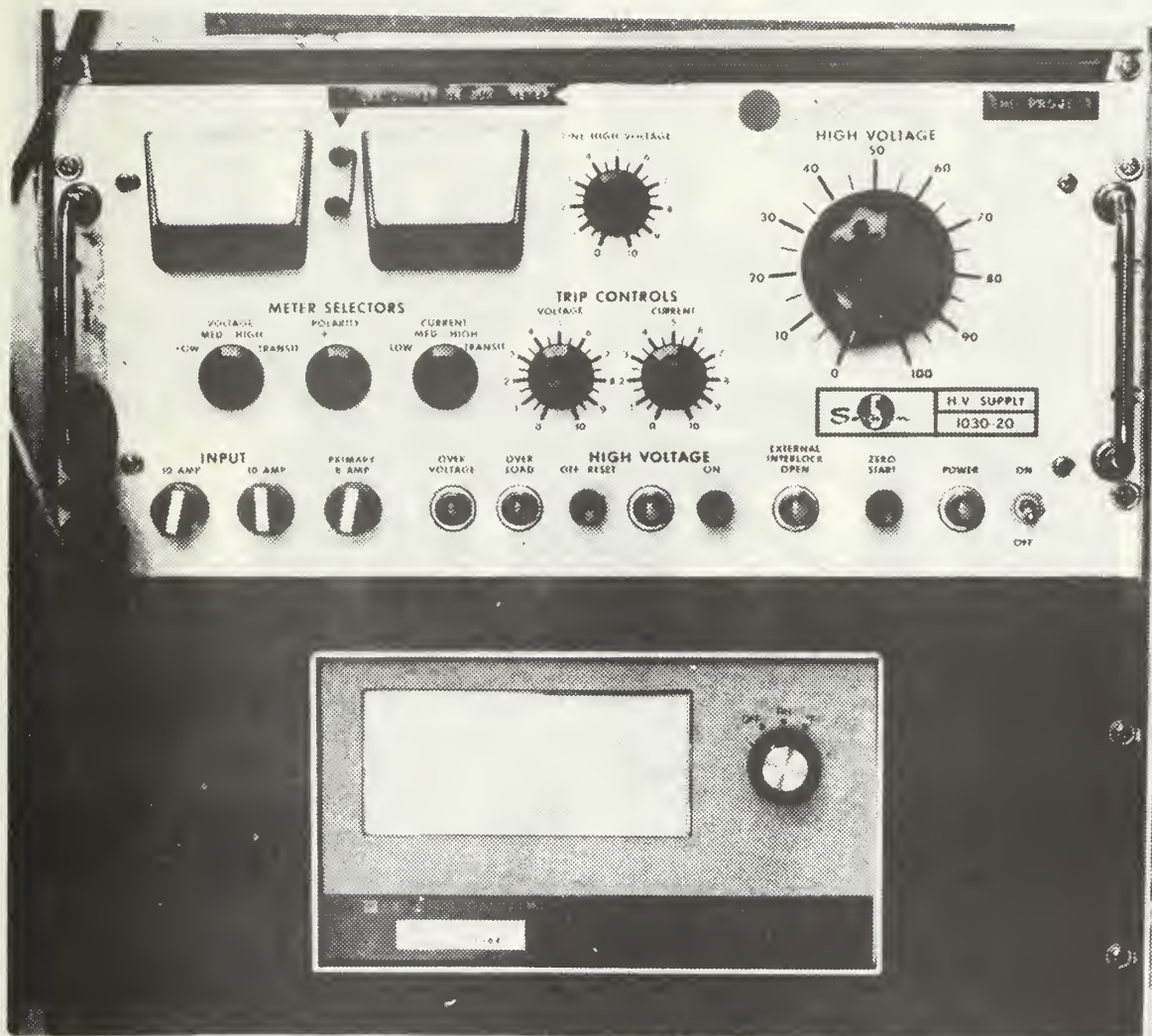


FIGURE 7. POWER SUPPLY



FIGURE 8. LABORATORY

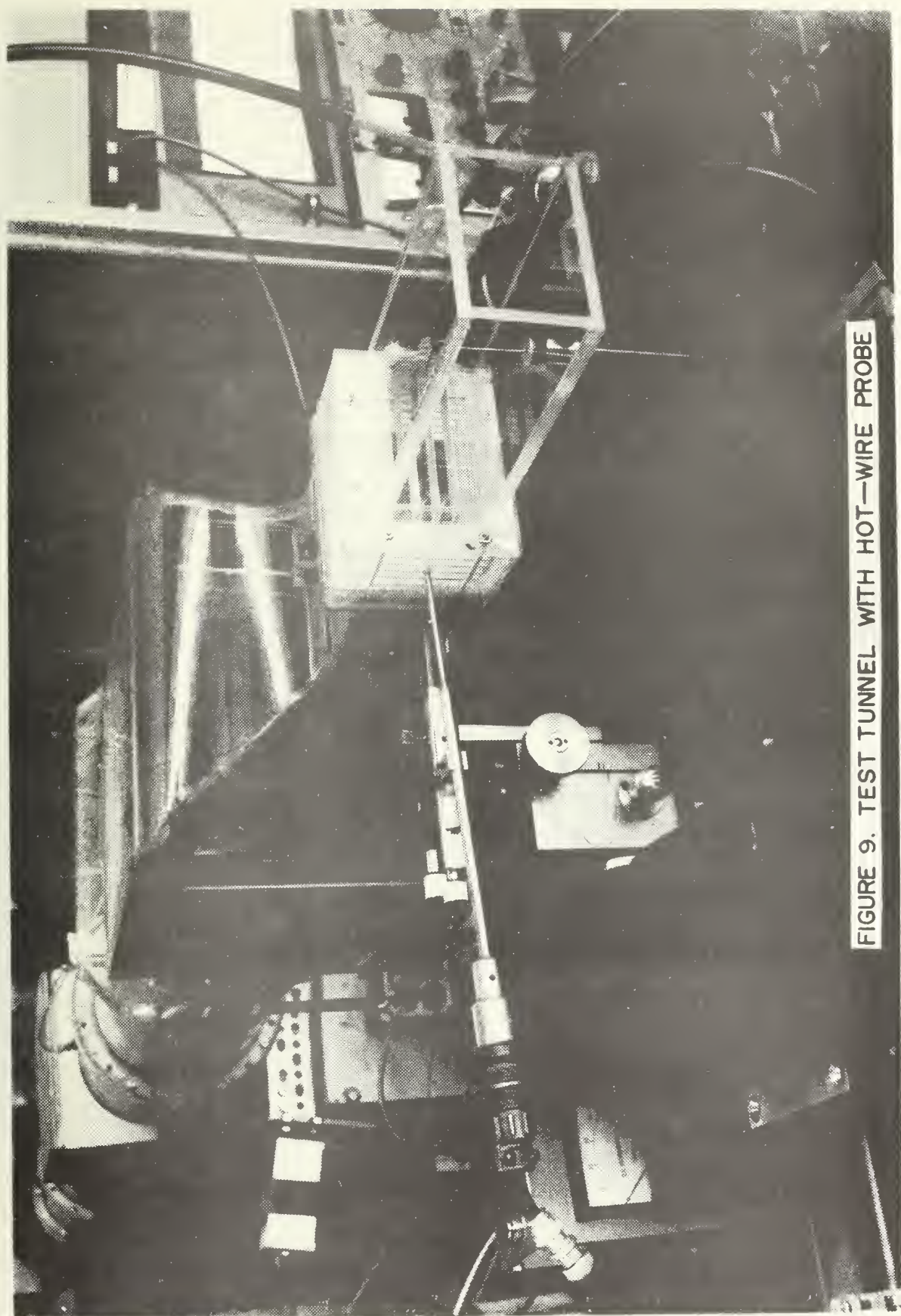


FIGURE 9. TEST TUNNEL WITH HOT-WIRE PROBE

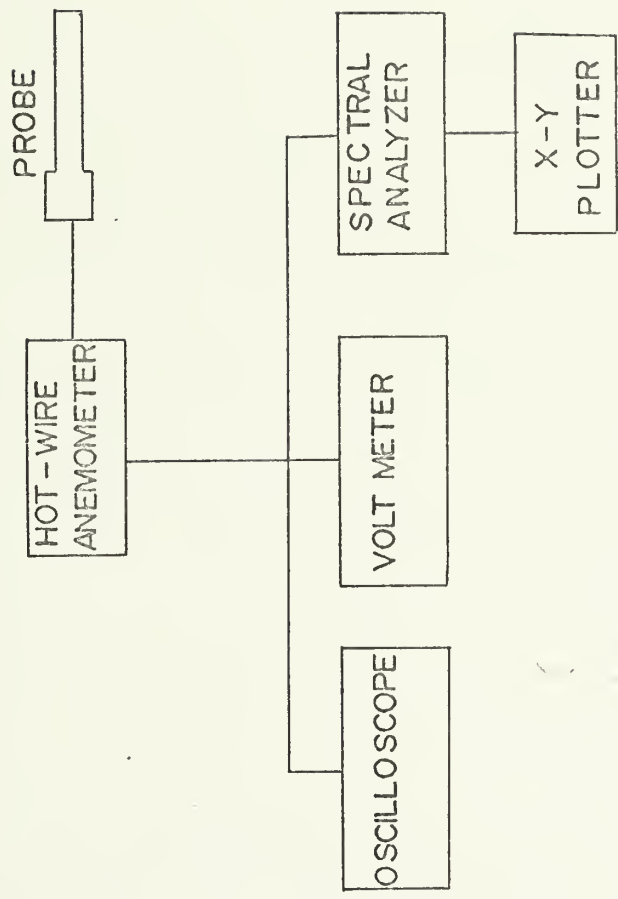


FIGURE 10. BOX DIAGRAM OF TURBULENCE DATA COLLECTION SYSTEM

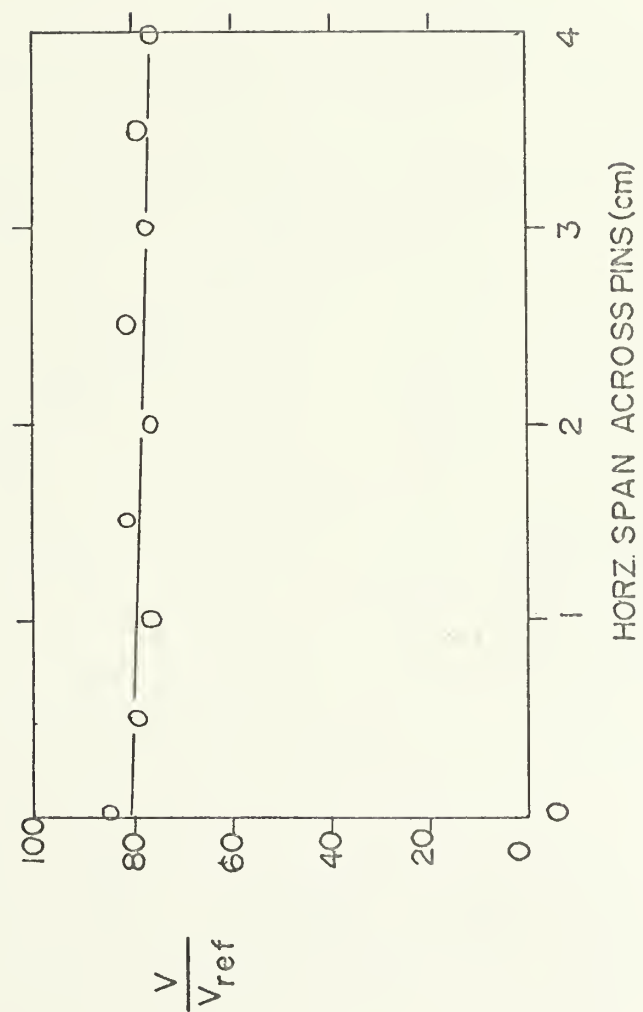


FIGURE II.
VELOCITY TRAVERSE

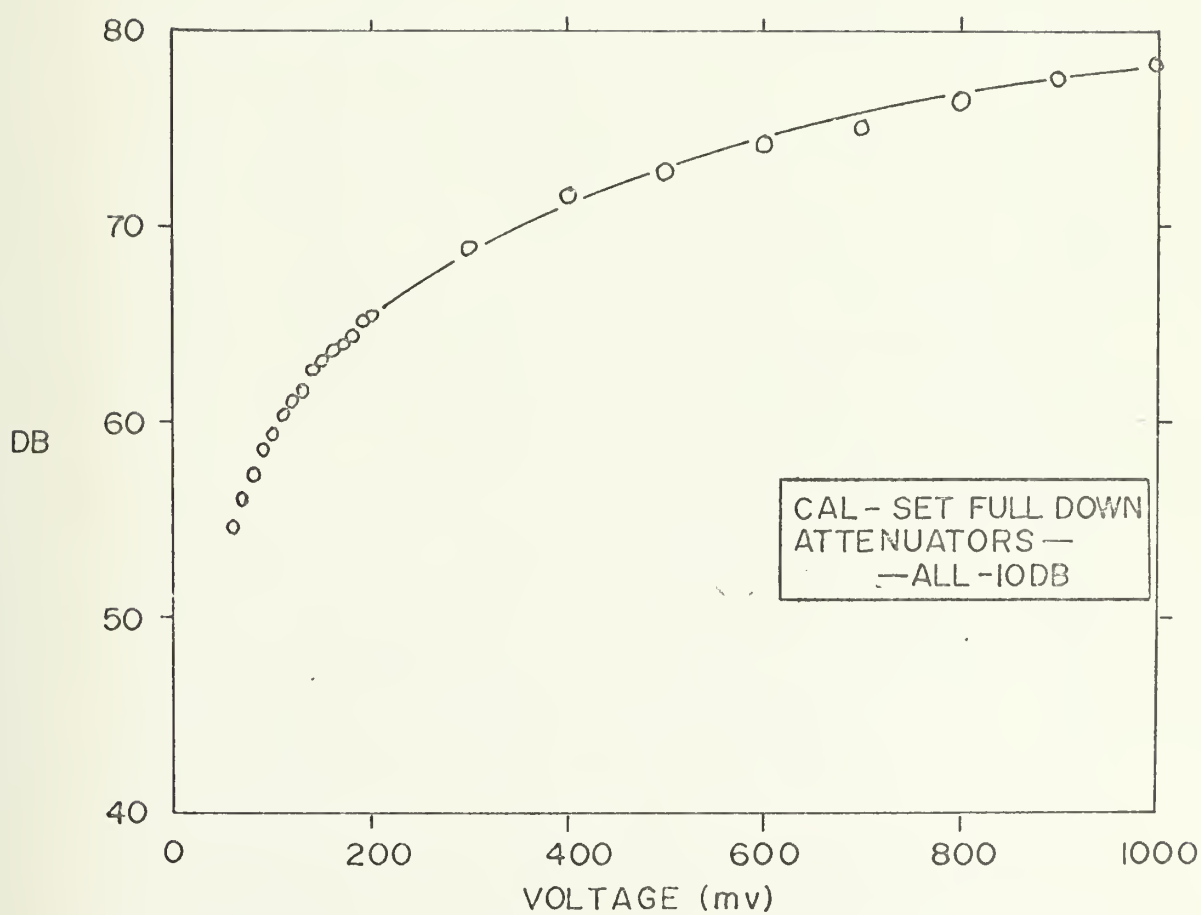


FIGURE 12. CALIBRATION OF RMS DETECTOR

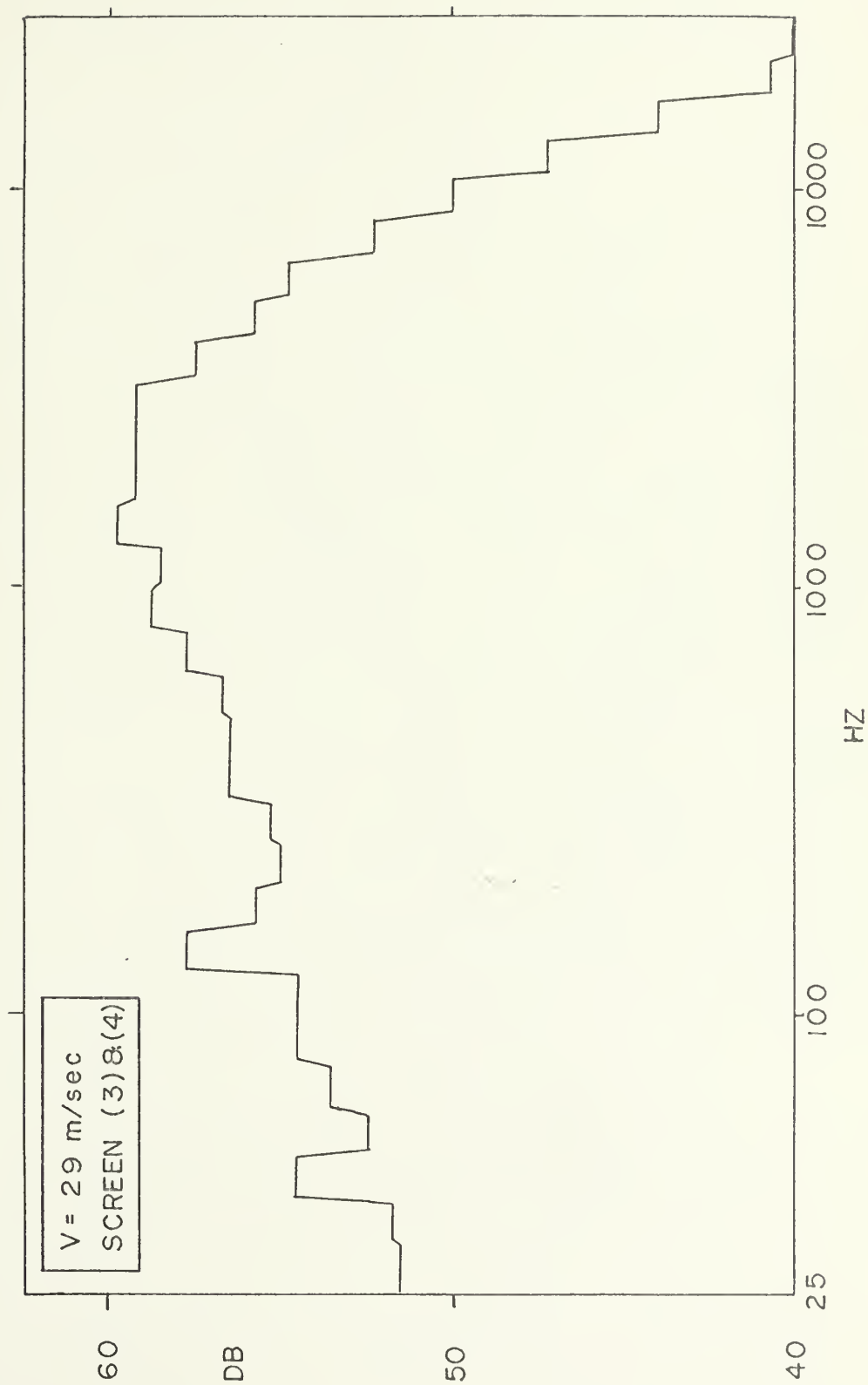


FIGURE 13. SAMPLE OF SPECTRAL OUTPUT

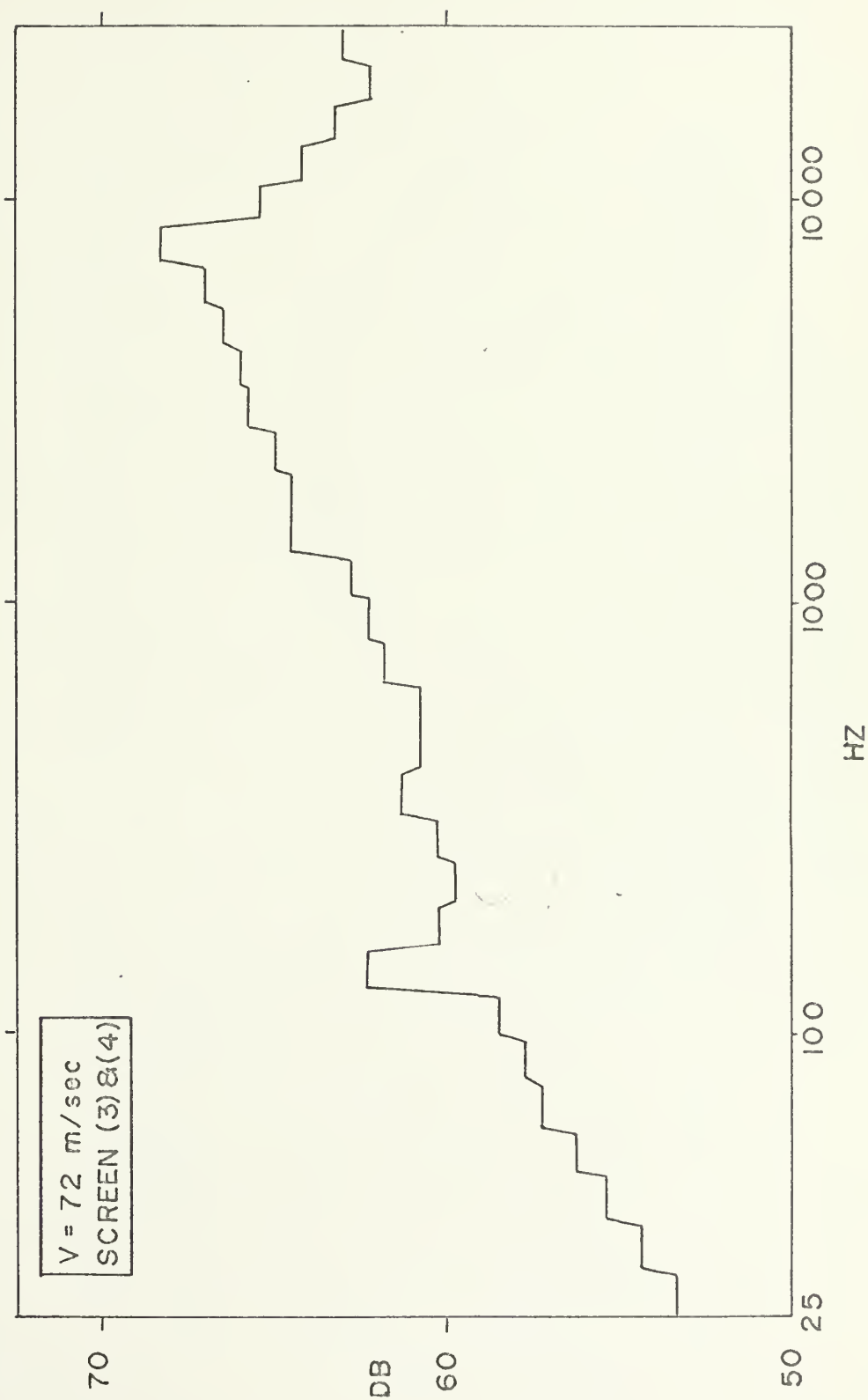


FIGURE 14. SAMPLE OF SPECTRAL OUTPUT

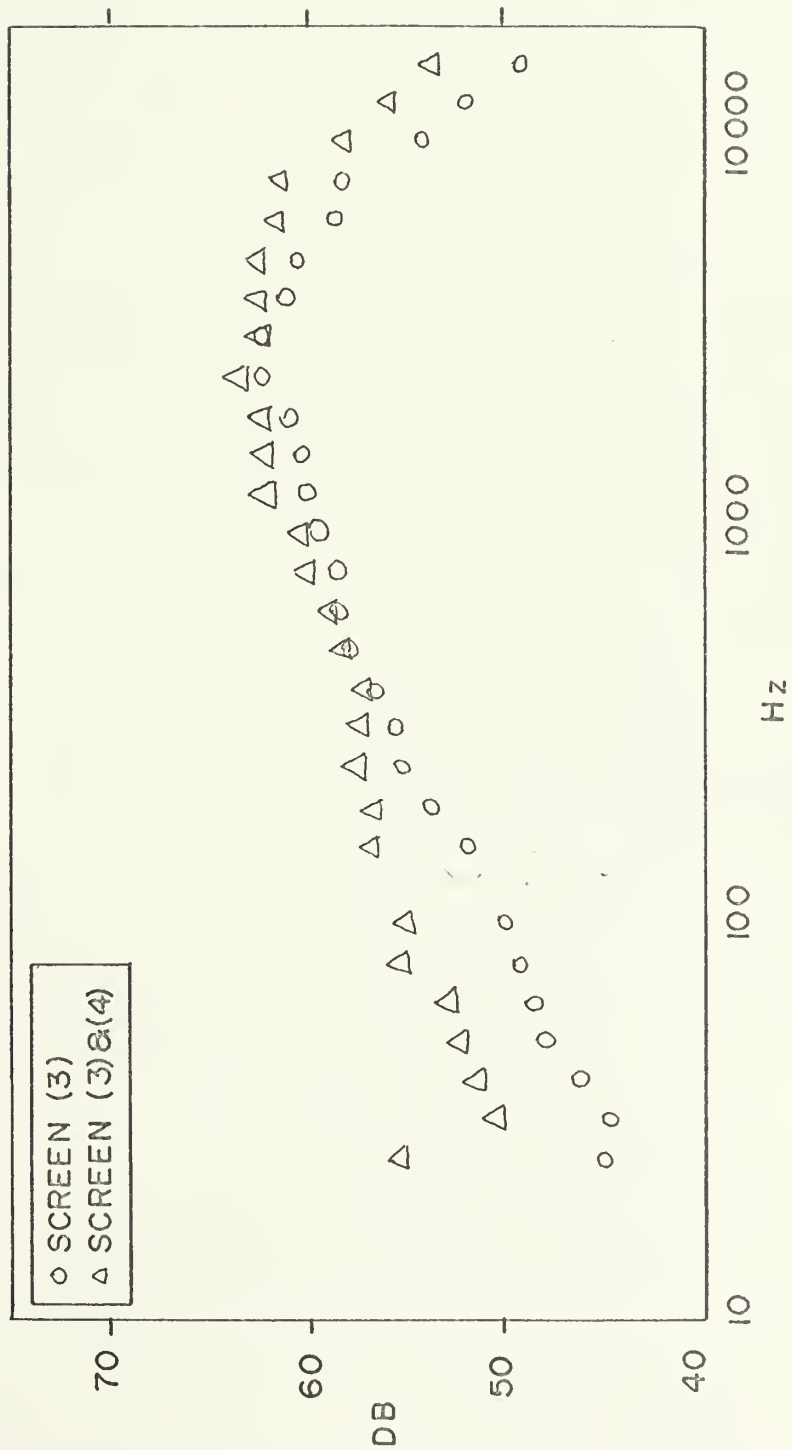


FIGURE 15.
SPECTRAL DISTRIBUTION ($V=50$ m/sec)

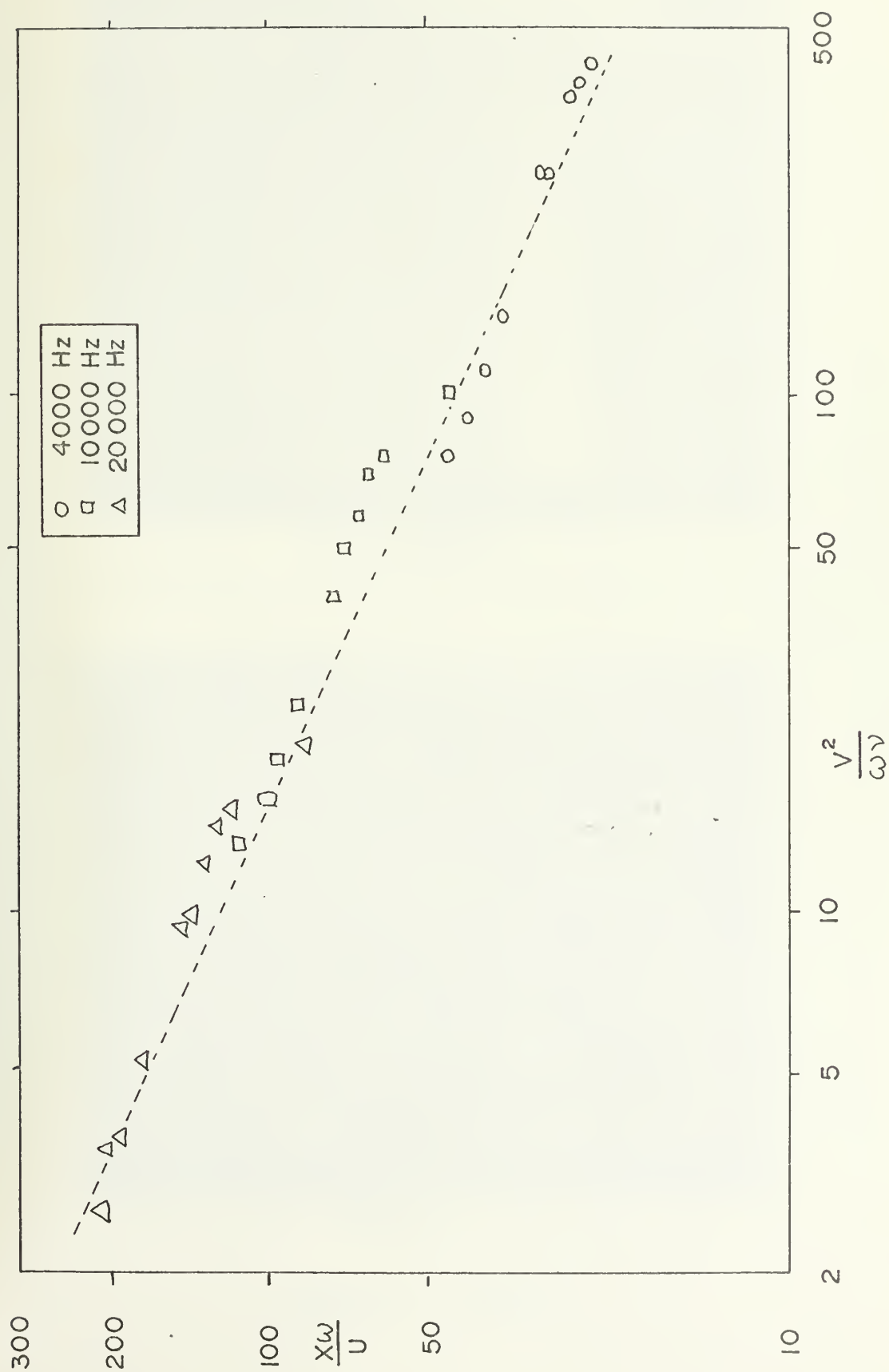
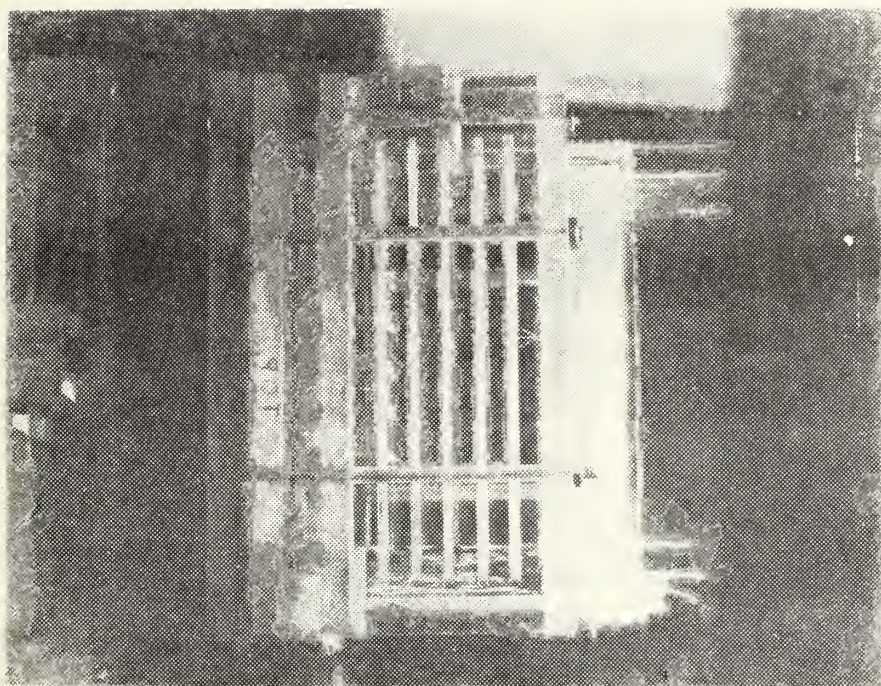
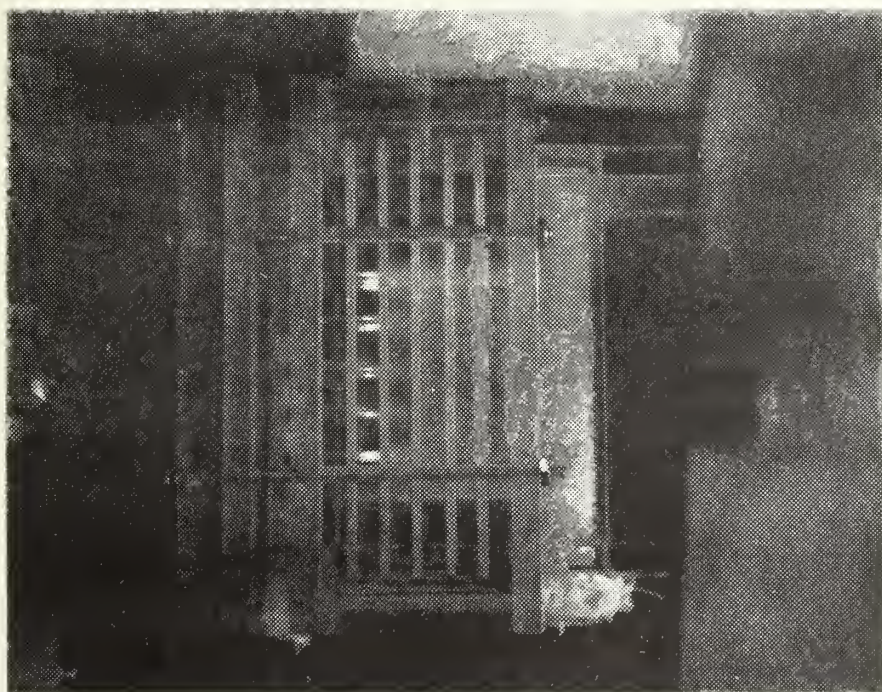


FIGURE 16. CORRELATION OF TURBULENCE DATA



NO CORONA



CORONA

FIGURE 17. CORONA

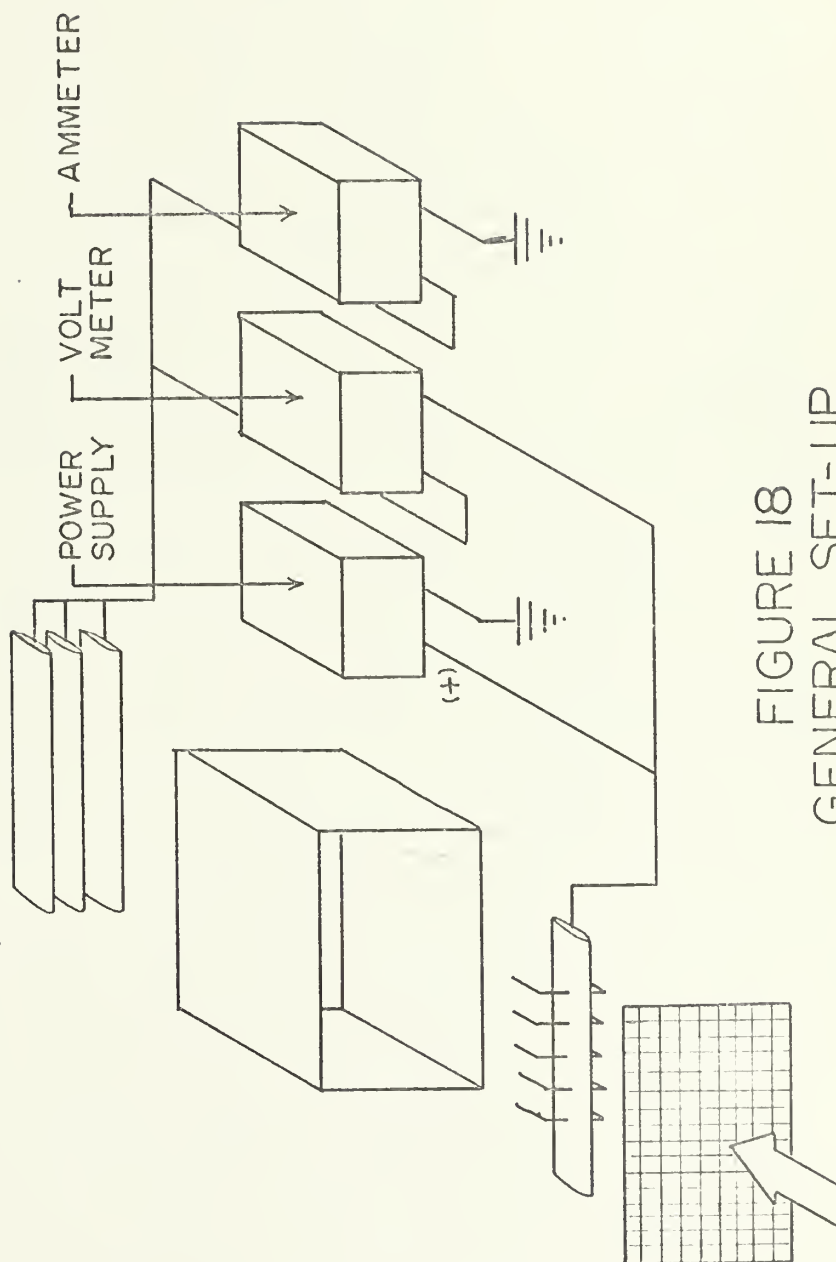


FIGURE 18
GENERAL SET-UP

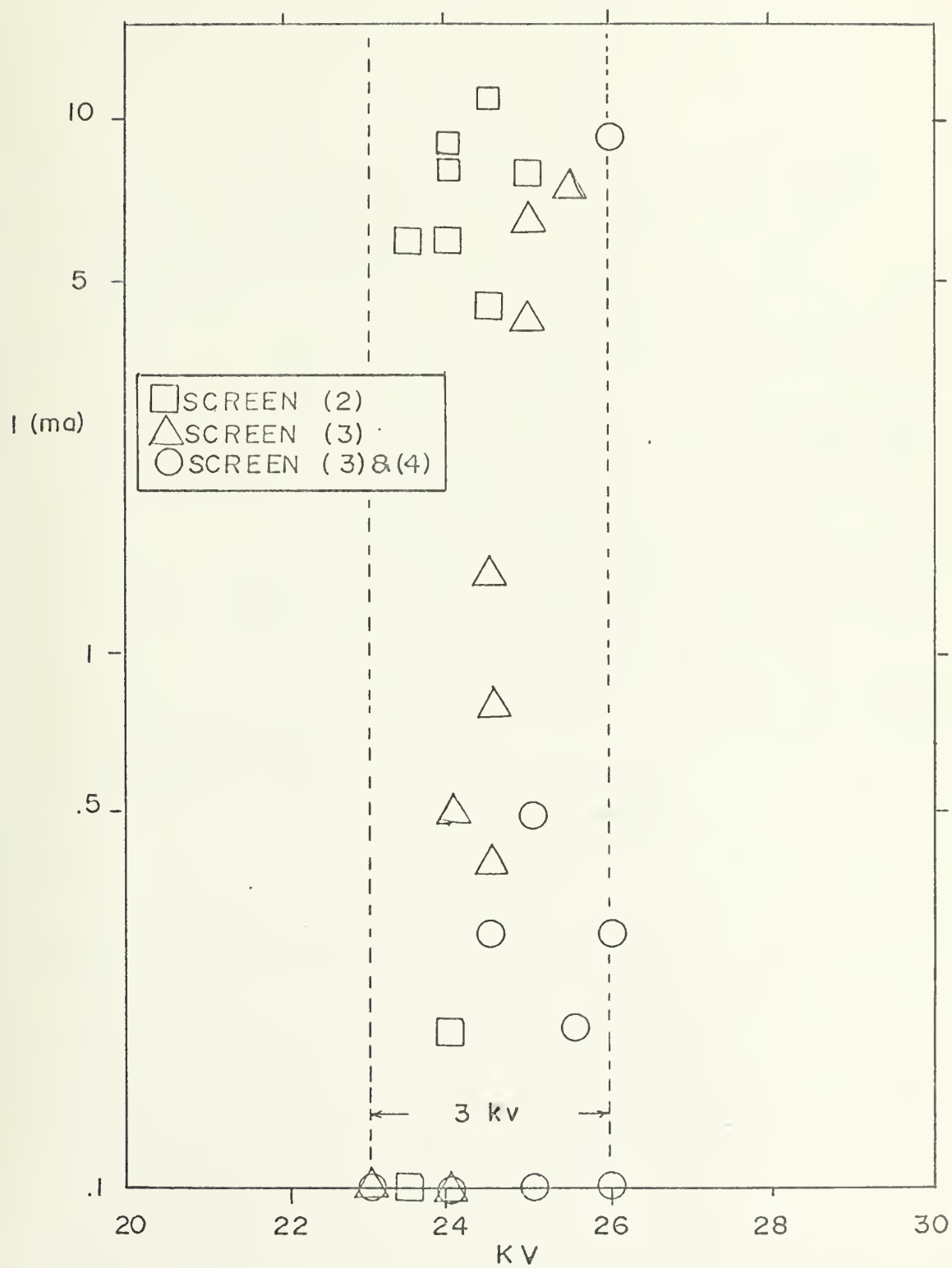


FIGURE 19.
CURRENT VS VOLTAGE

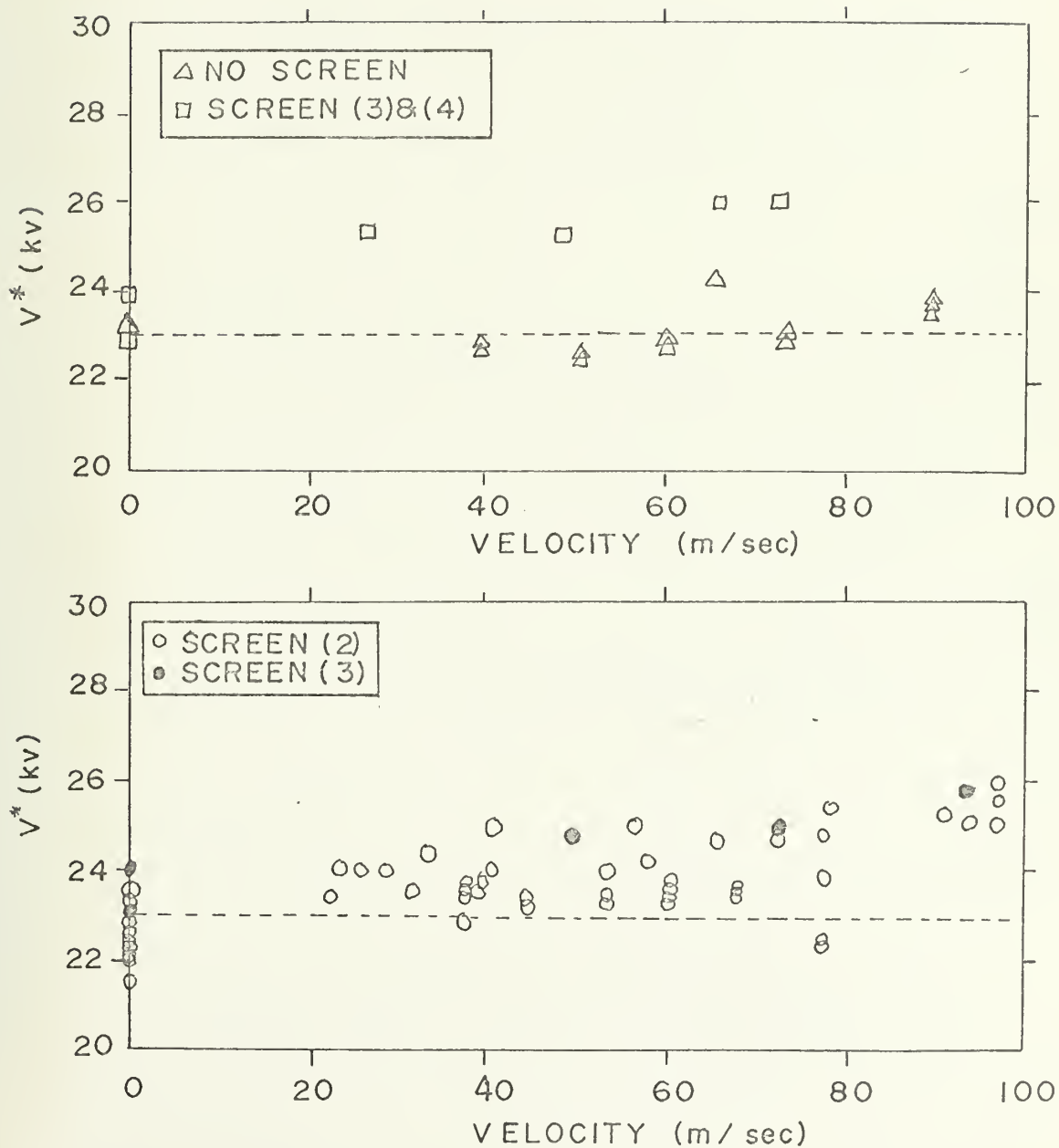


FIGURE 20.
BREAKDOWN VOLTAGE VS FLOW VELOCITY

APPENDIX A

MODEL OF THE PHENOMENA

This model involves the stabilization of the electric discharge by highly turbulent flow. It is felt that the phenomenon is brought about by two effects, convection and mixing, these effects act as follows:

(1) Convection

The mean flow velocity adds to the ion drift velocity.

This effect does not act on the breakdown voltage but increases the current by speeding up the ions. Mathematically, the effect may be expressed as follows:

$$I = \rho_e A (V_d + U)$$

The mean velocity of the flow simply adds to the drift velocity.

(2) Mixing

Mixing has two effects. First, because of mixing a longer path must be ionized for breakdown to occur. Thus the breakdown voltage is raised. Second, mixing causes diffusion of the space charge building up at the anode.

This diffusion reduces the charge density (ρ_e). A critical value of the charge density exists (ρ_{ec}), above which arcing occurs. Mixing allows a ρ_e very close to

ρ_{e_c} to exist over a larger area and thus permits an increase in current. Mathematically the effect acting on current can be described as follows:

Gauss' Law States:

$$\nabla \cdot E = \rho_e / \epsilon_o$$

This equation as stated below defines E_c and ρ_{e_c}

$$\nabla \cdot E_c = \rho_{e_c} / \epsilon_o$$

As in part one

$$I = \rho_e A (V_d + U)$$

Mixing allows a larger area (A_m) and the current equation becomes

$$I_m = \rho_e A_m (V_d + U)$$

Since ρ_e and ($V_d + U$) are somewhat constant,

$$I_m > I.$$

APPENDIX B

CALCULATION OF EDDY SIZE

The measured frequency of the turbulence cannot be applied directly to the calculation of δ_e . Eddies, sometimes called turbulence balls, move with the stream and thus a correction factor must be applied to data taken at a fixed point. This is done as follows:

$$\omega_e = \frac{V}{U} \omega_m$$

$$\omega_e = \frac{V}{\pi \delta_e}$$

$$\therefore \delta_e = \frac{V}{\pi \omega_e}$$

$$\delta_e = \frac{U}{\pi \omega_m} \left(\frac{V}{U} \right)^2$$

Example:

$$\omega_m = 8 \text{ kHz}$$

$$V = 0.065 \text{ volt}$$

$$U = 1.7 \text{ volt} = 19.9 \text{ m/sec}$$

$$\delta_e = (19.9) (8000)^{-1} (0.065/1.7)^2 = 1.16 \times 10^{-6} \text{ m}$$

$$R_e = \left(\frac{V}{\delta_e} \right) \left(\frac{V}{U} \right)^{-1} = 1 \quad \left(\text{Figure 21 shows the variation of } R_e = 1 \text{ with velocity} \right)$$

$$\delta_{R_e} = (1) (\mathcal{V})/V = (16.88 \times 10^{-5})(2.49)^{-1} = 2.07 \times 10^{-5} \text{ m}$$

δ_{R_e} and δ_e are within one order of magnitude.

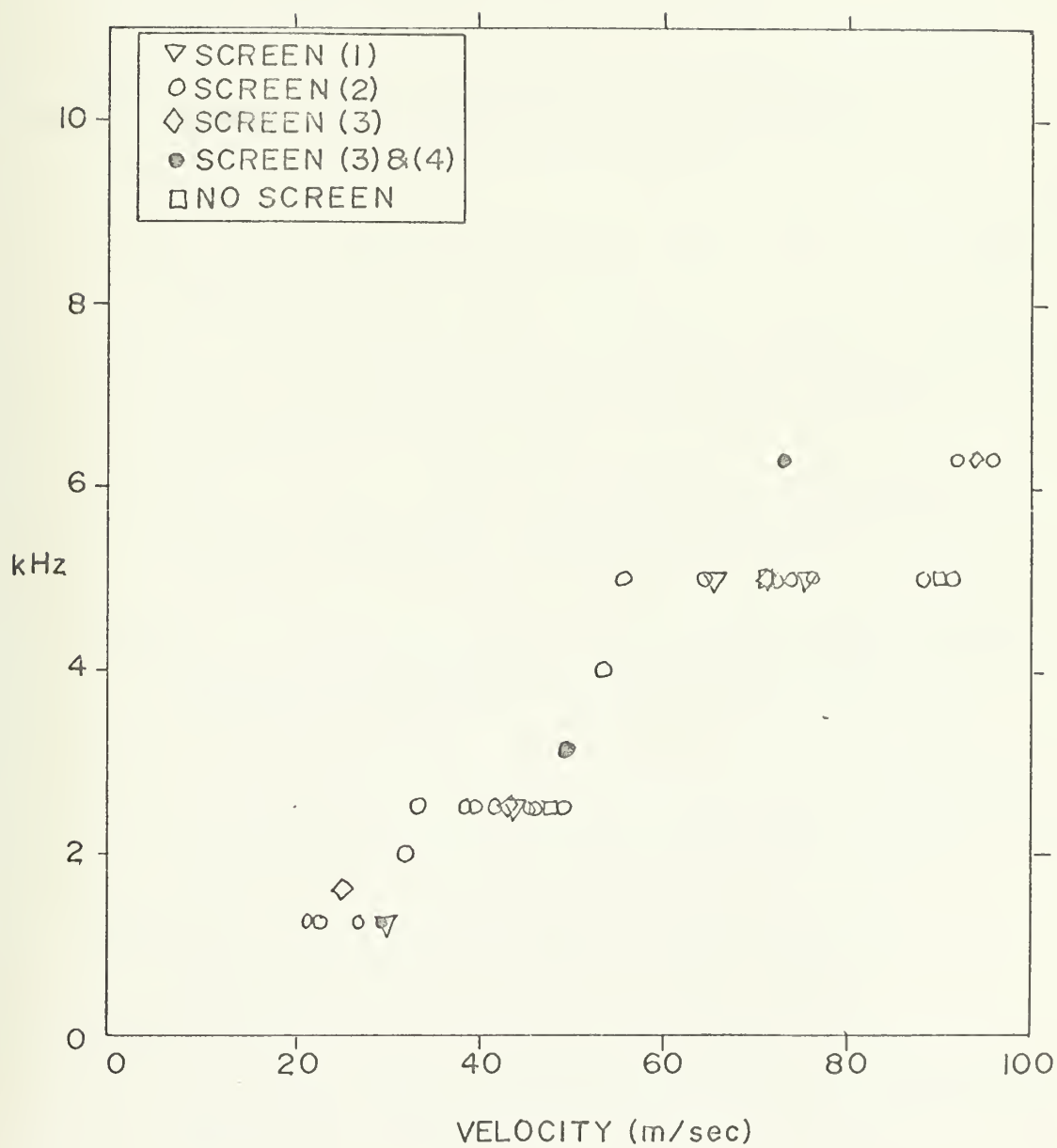


FIGURE 21.
FREQUENCY VS VELOCITY FOR $Re(EDDY) \approx 1$

BIBLIOGRAPHY

1. Batchelor, G. K., The Theory of Homogeneous Turbulence. Cambridge At The University Press, 1960.
2. Biblarz, O., EHD Research, Naval Postgraduate School Report NPS-57Z1121A, December 1968
3. Clark, P. O., Design Considerations For High Power Laser Cavities. AIAA paper number 72-708, American Institute of Aeronautics and Astronautics, New York 1972.
4. Cobine, J. D., Gaseous Conductors. Dover Pub., New York, 1958.
5. Davis, J. W. and Brown, C. O., Electric Discharge Convection Lasers. AIAA Paper 72-722, American Institute of Aeronautics and Astronautics, New York, 1972.
6. Demetriades, et. al., Influence of Controlled Turbulence on Gaseous Discharges. Eleventh Symposium on Engineering Aspects of MHD, Cal. Tech., March 1970, pg. 64-69.
7. Eckbreth, A. C. and Blaszk, P. R., Closed-Cycle CO₂ Laser Discharge Investigations. AIAA Paper number 72-723. American Institute of Aeronautics and Astronautics, New York, 1972.
8. Hinze, J. O., Turbulence An Introduction To Its Mechanics and Theory. McGraw-Hill Inc., New York, 1959.
9. Landau, L. D. and Lifshitz, E. M., Fluid Mechanics. Institute of Physical Problems USSR Academy of Sciences. Pergamon Press Ltd., Great Britain, 1966.
10. Pan, Yu-Li, Bernhardt, A. F., and Simpson, J. R., Construction And Operation of A Double-Discharge TEA CO₂ Laser. The Review of Scientific Instruments, Volume 43 number 4, 1972.
11. Schlichting, H., Boundary Layer Theory. McGraw-Hill Inc., New York, 1968.

12. Sutton, G. W., and Sherman, A., Engineering Magneto-hydrodynamics. McGraw-Hill Inc., New York, 1965.
13. Tennekes, H. and Lumley, J. L., A First Course In Turbulence. The MIT Press, Cambridge, Massachusetts, 1972.

INITIAL DISTRIBUTION LIST

	No. Copies
1. Defense Documentation Center Cameron Station Alexandria, Virginia 22314	2
2. Library Naval Postgraduate School Monterey, California 93940	2
3. Professor O. Biblarz Department of Aeronautics Naval Postgraduate School Monterey, California 93940	4
4. LT Robert E. Nelson, USN 922 Lake Terrace Pensacola, Florida 32505	1
5. Dr. R. W. Bell Chairman Department of Aeronautics Naval Postgraduate School Monterey, California 93940	1

Unclassified

Security Classification

DOCUMENT CONTROL DATA - R & D

(Security classification of title, body of abstract and indexing annotation must be entered when the overall report is classified)

ORIGINATING ACTIVITY (Corporate author)

Naval Postgraduate School
Monterey, California 93940

2a. REPORT SECURITY CLASSIFICATION

2b. GROUP

REPORT TITLE

Electric Discharge Stabilization by a Highly Turbulent Flow

DESCRIPTIVE NOTES (Type of report and, inclusive dates)

Master's Thesis; June 1973

AUTHOR(S) (First name, middle initial, last name)

Robert E. Nelson

REPORT DATE

June 1973

7a. TOTAL NO. OF PAGES

55

7b. NO. OF REFS

13

CONTRACT OR GRANT NO.

9a. ORIGINATOR'S REPORT NUMBER(S)

PROJECT NO.

9b. OTHER REPORT NO(S) (Any other numbers that may be assigned this report)

DISTRIBUTION STATEMENT

Approved for public release; distribution unlimited.

SUPPLEMENTARY NOTES

12. SPONSORING MILITARY ACTIVITY

Naval Postgraduate School
Monterey, California 93940

ABSTRACT

This work investigates an electric discharge operating in a turbulent flowing gas. Electric-discharge convection lasers are driven by such a discharge and any limit on discharge power will be a limit on the laser output. It has been observed that turbulence tends to allow more power to be applied but the exact mechanisms involved are not fully understood. To examine this phenomenon an air flow apparatus was fabricated that allowed control of flow rate, turbulence level, and discharge power. Turbulence data were taken with a hot-wire connected to a spectral analyzer. Discharge power consumption and breakdown voltage were recorded as a function of flow rate and turbulence spectrum. Results showed that with even a small flow rate discharge, current was raised by about a factor of two, with turbulence by about a factor of four; and with a large flow rate (100 m/sec) and strong turbulence, by about a factor of 100. Power at this last condition was raised by a factor of 200 over the no-flow case.

Security Classification

FORM 1473 (BACK)
1 NOV 68
01-807-6821

Thesis
N3663 Nelson
c.1

144244

Electric discharge
stabilization by a
highly turbulent flow.

Thesis
N3663 Nelson
c.1

144244

Electric discharge
stabilization by a
highly turbulent flow.

J thesN3663

Electric discharge stabilization by a hi



3 2768 001 89885 1

DUDLEY KNOX LIBRARY